Measurement 153 (2020) 107415

Contents lists available at ScienceDirect

Measurement

journal homepage: www.elsevier.com/locate/measurement

Non-Contact vehicle Weigh-in-Motion using computer vision

Maria Q. Feng, Ryan Y. Leung *, Casey M. Eckersley

Department of Civil Engineering and Engineering Mechanics, Columbia University, New York, NY 11027, USA

ARTICLE INFO

Article history:
Received 31 July 2019
Received in revised form 5 December 2019
Accepted 16 December 2019
Available online 20 December 2019

Keywords:
Computer vision
Weigh-in-Motion (WIM)
Tire
Truck
Deformation measurement

ABSTRACT

Heavy vehicles must be closely monitored to prevent fatigue-induced deterioration and critical fractures to transportation infrastructure. This paper introduces an innovative computer vision-based non-contact vehicle weigh-in-motion method and presents a proof-of-concept study. The method is based on simple physics that tire-roadway contact force equals the contact pressure multiplied by the contact area. The area can be estimated by measuring tire deformation parameters such as tire-roadway contact length and tire vertical deflection using computer vision, while tire pressure can be streamed from on-board sensors. To demonstrate the feasibility of this method, a computer vision system was developed and experiments were conducted involving empty and fully loaded concrete trucks and a sport utility vehicle. Results show high accuracy of vehicle weight estimation, demonstrating the potential of this computer vision-based method as a non-contact means for weighing vehicles in motion.

1. Introduction

Overloaded vehicles have become a serious concern to civil infrastructure safety across the globe [1]. Heavy trucks can, for example, cause severe damage and deterioration leading to bridge components fatigue and failure [2]. Because of this negative impact on serviceability and durability of civil infrastructure, they present a significant risk. Hence, determining a vehicle weight, especially an overweight truck, is essential for infrastructure owners, law enforcements, and general public [3].

Existing methods to measure vehicle weight include static weighing and pavement-based weigh-in-motion (WIM) platforms.

The static weighing has been considered as the standard method for weight limit enforcement. Although static weighing may produce accurate results, the implementation is time-consuming and uneconomical, often requiring permanent installation of the systems. Additionally, such method requires interceptions of selected trucks, causing traffic disruptions. Statistics show that the average timespan of being selected and checked twice for one given truck was 30 years [3]. For such reason, WIM techniques are developed and introduced to address the limitations of static weighting.

Pavement-based WIM systems, similar to static weighing, use sensors/devices installed on the pavement and include both low-speed systems (LS-WIM) and high-speed WIM systems (HS-WIM) [3,4]. LS-WIM uses force sensing technologies like wheel or axle scale plates, capacitive strips, and piezo-electric cables [3–6]. While LS-WIM addresses some inadequacies of static weighting, the technique still requires selected trucks to enter a controlled area and to wait in queue. To eliminate unnecessary slow-downs, HS-WIM allows vehicles to travel at normal speed, utilizing bending plates and load cells instrumented with sensors or multiple strip sensors [3,4,7]. Both LS-WIM and HS-WIM systems, however, remain costly and require traffic closures during extensive installations and frequent maintenance [4,8]. In addition, the accuracy depends greatly on the quality of and the number of sensors, road surface roughness, and other external factors that prevent the system from being implemented or approved for enforcement purposes [3,8].

Bridge WIM systems (B-WIM), different from existing methods, were introduced to use an instrumented bridge as a scale to estimate vehicle weights. Moses' algorithm is considered the basic framework for B-WIM [9]. Much research on B-WIM was subsequently carried out. Richardson et al. gave a thorough review of overall development from traditional WIM (pavement-based WIM) to B-WIM [4]. A review by Yu, Cai, and Deng focused on the fundamental methodologies and the field implementation of B-WIM [5]. Lydon et al. also provided a summary of key challenges experienced during system implementations [10]. However, B-WIM still necessitates prior knowledge of the bridge structural parameters (e.g. stiffness) and costly sensor instrumentation of the bridge [11,12]. Therefore, a more reliable and cost-effective WIM method independent of the bridge condition is demanded.

The emerging computer vision technology has found successful applications in many areas including structural vibration

* Corresponding author.
E-mail address: yl3649@columbia.edu (R.Y. Leung).

https://doi.org/10.1016/j.measurement.2019.107415
0263-2241/

measurement and health monitoring. The unique advantages such as low cost, non-contact, and non-destructive implementation make the computer vision a superior choice over the conventional sensors. Feng and Feng conducted an extensive review on computer vision sensor technologies and their applications for structural health monitoring [13]. In the field of WIM, McKay et al. used computer vision to approximate the vehicle mass from engine torque-induced frame twisting [14]. Ojio et al. and Capriani, O'Brian, and Blacoe utilized a roadside camera to explore the possibility of vehicle axle identification [15,16]. However, the question remains: can computer vision remotely extract sufficient information to accurately estimate the weight of a traveling vehicle?

This proof-of-concept research presents an innovative computer vision-based non-contact WIM system, in which the vehicle contact force of each tire is computed as a product of the tire contact area (acquired using computer vision) and the tire pressure. The weight of the vehicle is simply the sum of all the tire contact forces. In order to evaluate the feasibility and accuracy of this vision-based WIM method, experiments have been conducted on stationary and moving vehicles including a sport utility vehicle (SUV) and heavy trucks. Such computer vision-based non-contact WIM method will have significant advantages over the traditional static weighing and other WIM methods.

2. Methodology and computer vision system

Despite the complexity of a vehicle, estimating the weight of a vehicle fundamentally requires only two vehicle parameters—tire-roadway contact area and contact pressure. The contact area of a vehicle tire, also referred to as the tire footprint, is the region of tire in contact with the road, which is illustrated in Fig. 1. The tire force exerted on the roadway surface equals the tire-roadway contact pressure multiplied by the corresponding tire contact area. The vehicle weight is the sum of all the tire forces as

$$W = \sum_{i=1}^{N} P_i \cdot A_i \tag{1}$$

where W is the weight of the vehicle, N is the number of the tires of the vehicle, P_i is the tire-roadway contact pressure and A_i the tire-roadway contact area of the i-th tire.

In this study, the tire-roadway contact pressure is assumed to be identical to the tire internal inflation pressure. The vehicle load applied to the wheel causes the tire to deflect until the average tire contact pressure is balanced by the tire internal inflation pressure [17]. Inflation pressure is the effect of pressurized air that increases the stiffness of the tire [18]. Many studies have been carried out to study the correlation between the contact pressure and inflation pressure of a tire [19,20], and experimental data showed that average tire contact pressure at the same loading condition is typically identical to and rarely exceed the inflation pressure [21]. Hence, in this study, the tire inflation pressure is used as the tire-roadway contact pressure and it is simply referred to as the tire pressure

2.1. Computer vision-based non-contact WIM system

A computer vision-based WIM system has been developed for non-contact weight estimation of moving vehicles according to Eq. (1). A schematic of the weight estimation procedure is shown in Fig. 2. First, the computer vision system acquires tire contact area. A roadside camera captures images of a passing tire (as shown in Fig. 1). Computer vision techniques are used to (1) measure the tire deformation parameters including the tire-roadway contact length or tire's vertical deflection and (2) identify the tire make/model from sidewall markings to acquire the tire information from a database such as the tire width and the manufacturer recommended tire inflation pressure. The scaling factor (SF), which will be explained in-depth in Section 2.3, needs to be determined in order to convert the measurement in pixel to physical dimensions in, for example, inches.

For accurate weight estimation, actual tire pressure measured by the vehicle's on-board tire pressure monitoring system (TPMS) should be used. Commercial trucks that are manufactured after 2012 are mandated to have onboard TPMS in order to maintain manufacturer suggested tire pressure for optimal mobility, safety, and fuel efficiency [22,23]. When real-time tire pressure information is unavailable, a manufacturer suggested tire inflation pressure is utilized used based on the tire make/model identified by the computer vision. Recent technology has also made it possible to acquire tire inflation pressure information wirelessly [24].

Integrating these two pieces of information—tire contact area and tire pressure, the vehicle weight can be estimated according to Eq. (1). Proper longtitude and lateral load balance are undoubtedly essential. Vehicles, especially heavy trucks, require proper load balance to ensure economic efficiency, safety and, not to mention, compliance to the regulations [25]. Therefore, it is valid to assume a well-maintained vehicle to have symmetrical lateral weight distribution. The total weight can be obtained by doubling the one-sided weight.

In order to investigate the feasibility of this methodology, a computer vision-based non-contact WIM system has been prototyped, which consists of a camera (Sony SLT-A77 digital SLR camera equipped with a Tamron AF 70–200 mm f/2.8 Macro Lens) and a laptop computer. The camera can be placed on the roadside, as shown in Fig. 3. Fig. 4 shows a tire image captured by this camera

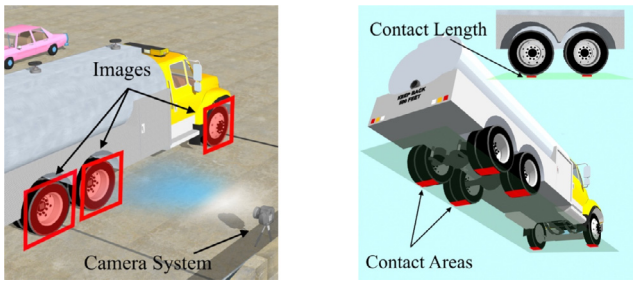

Fig. 1. Non-contact computer vision-based WIM system.

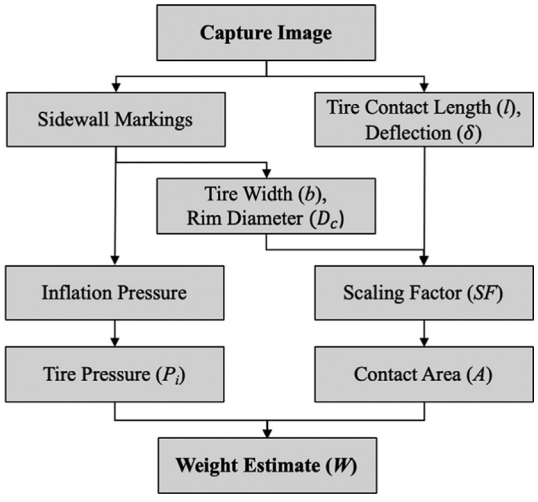

Fig. 2. Processing algorithm of non-contact computer vision-based WIM system.

Fig. 3. Camera setup for the field tests.

Fig. 4. Tire image of a truck at highway speed.

at the shutter speed of 1/8000 on the side of the interstate highway I-495. The truck was traveling approximately 65 mph. Future study will also consider the use of high-resolution video camera with slow motion capability.

2.2. Methods for computing tire contact area

The contact area of a tire is the region across which forces are transmitted between the vehicle and the roadway as shown in Fig. 1. The shape of the contact area varies depending on the tire operating conditions, tire cross section shape, and its structure. Automotive tire, especially heavy truck tire (which traditionally has deeper treads), differs from the treadless aircraft tire, and truck tire tends to have parallel sides leading to a nearly rectangular or squared contact area [17,18,26]. Fig. 5 shows a schematic of a typical heavy truck tire footprint and a side view of the deformed tire, indicating the tire-roadway contact length, width, and tire vertical deflection [27].

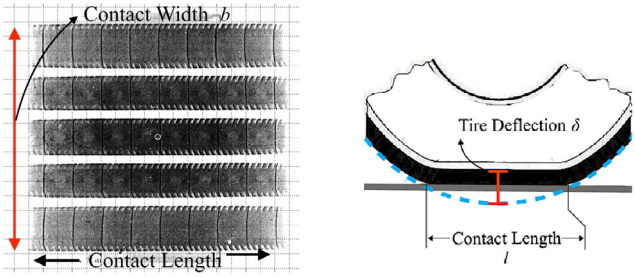

Fig. 5. Typical truck footprint (left) and tire deformation parameters (right).

Many studies have been performed on tire-roadway contact mechanics and several equations have been proposed to compute the contact area. Table 1 summarizes three major methods and equations for calculating the tire contact area [28–31]. The notations l, b, and δ represent the contact length, contact width, and tire deflection respectively. The rectangular method simply multiplies the contact length l and width b to yield the tire contact area. The deflection method utilizes the tire defection δ, which can also be measured by computer vision as illustrated in Fig. 5. C_3 is a constant coefficient computed empirically based on specification provided by the tire manufacturer for a given tire, D_p is calculated using section width and height of the given tire cross-section in meter, and D_c is the tire overall diameter in meter [30]. Note that the rectangular method requires the tire width to compute the tire contact area, while neither the defection nor the oval method requires the tire width information.

This study investigates these three methods for computing the tire-roadway contact area by using the computer vision to measure the tire contact length l and the tire deflection δ. The tire width b can be obtained once the make and model of the tire are identified by the computer vision.

2.3. Image rectification and scaling factor for measurement

In order to accurately measure the tire deformation parameters including the tire-roadway contact length and the tire defection from a tire image, the image must be first rectified to correct any perspective and tangential distortions due to non-perpendicular angle of the camera optical axis to the tire. Fig. 6 (left) displays the raw image of the tire with major radius and minor radius identified for rectification, and the rectified images of the tire are shown in the right of the figure. The vehicle wheel rim and the edge of the tire rubber are considered two concentric circles, without any tire deflection. For the simplicity and practicality of the study, the roadway is assumed to be rigid and flat, meaning that there is no pavement deformation. Hence, all observed deflection is the tire deflection.

Using the rectified image, the tire contact length and the tire deflection are measured. In order to convert the pixel dimension in the image into physical dimension, a scaling factor needs to be determined. A practical calibration method developed by the first author and her team is adopted to compute the scaling factor (SF), by using a known dimension of an object in the image described in Eq. (2) as

$$SF = d_{known}/I_{known} \tag{2}$$

where d_{known} represents the known physical length of the object and I_{known} is the corresponding pixel length at the image plane of such object [13,32,33].

In this study, it is proposed to use diameter of the tire rim as the known physical length, because it is reasonable to assume that the rim is rigid, and the rim diameter is standardized and marked on the tire (which can be recognized by computer vision). All tires are required to bear tire codes or sidewall markings stating the tire brand, tire model, and other manufacturer's compliance codes [34]. An example of such markings is shown in Fig. 7, which indicates 425/65R22.5 KUMHO KMA02. The tire brand and model are

Table 1
Methods and equations for computing tire contact area.

Method	Equation	Reference
Rectangular	$A = b \cdot l$	–
Deflection	$A = (\pi/2) \cdot C_3 \sqrt{(D_p\delta - \delta^2)(D_c\delta - \delta^2)}$	[28–30]
Oval	$A = 1.9131 \cdot l^2$	[31]

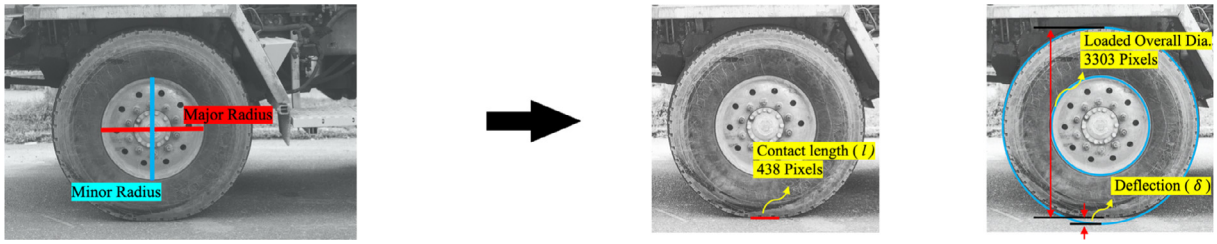

Fig. 6. Raw image (left), rectified image (middle) with contact length, and rectified image (right) with tire deflection.

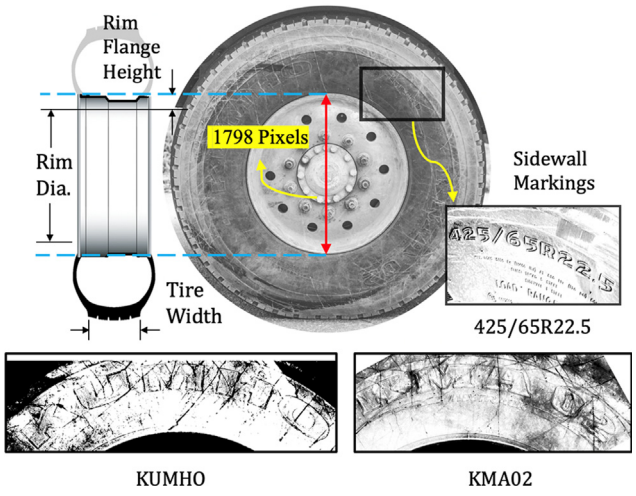

Fig. 7. Rim diameter in pixels, rim flange height, tire width, and sidewall markings.

identified as KUMHO KMA02. The first number is the tire section width (B) in millimeters, in this case 425mm. The second number is the aspect ratio of tire height (H) to section width. The letter R indicates the tire is radial construction, which dominates the tire market since its first introduction because of its efficiency for hauling. The last number is the rim diameter in inches, in this case 22.5 in. [17]. All essential information extracted from the captured image (tire section width, etc.) are tabulated in Table 2.

The scaling factor can then be calculated using the known tire rim diameter or overall diameter and their corresponding number of pixels at the image plane. Typical heavy truck tires feature a 20 mm rim flange height [35–39]. As shown in Fig. 7, adding twice of the rim flange height, i.e., 40 mm or 1.57 in, to the rim diameter 22.5 in to obtain the total physical length of the rim, and then counting the number of pixels 1798 of the corresponding length in the image, the scaling factor for the sample tire in Fig. 6 is calculated as $SF = (22.5 + 2 \times 0.787)/1798 = 0.0134\text{in./pixel}$.

2.4. Measured tire contact length and tire deflection

The tire contact length is the straight line of the deformed tire in contact with the roadway, which is measured from the rectified tire image. For the example tire image in Fig. 6, the tire contact length occupies 438 pixels in the image, which is converted to the physical length by multiplying the scale factor as $l = 438 \times 0.0134 = 5.87\text{in}$.

As shown in Fig. 6, the tire vertical deflection is computed as the overall diameter of the undeformed tire minus the diameter of the deformed (i.e. loaded) tire in the vertical direction. The overall tire diameter of tire is 45.90 in as listed in Table 2. The pixel length of the deformed diameter is 3303 pixels at image plane. Hence, tire deflection is obtained as $\delta = 45.90 - 3303 \times 0.0134 = 1.62\text{in}$.

The width of the contact area of a tire is defined by the width of the tire tread and has no correlation to the deflection of the tire [21,26]. Manufacturer data sheets similar to Table 2 often specify the tread width of a tire. However, if tire tread width is not specified, an empirical assumption is made. Typical design criteria recommend that tire tread width be at least 60% and at most 90% of the section width of the tire for optimal operation. Another guideline suggests a ratio of tread width to rim width to be between 1 and 1.3. Therefore, in this study, the mean (75%) is assumed [17,40–43]. The tread width for the tire in Fig. 6 is 13 in. Using the above assumption, 75% of the section width (17.3 in.) is 12.98 in., which is essentially equal to the actual tread width.

Once the tire contact length, width, and tire deflection are determined, the three methods outlined in Table 1 are utilized to compute the tire contact area.

3. Experimental validation

In order to investigate the feasibility of non-contact WIM methodology and to evaluate the accuracy of the computer vision system, numerous experiments were conducted. The following sections will deliver the experimental results, key validations, and brief discussions of each field test.

To evaluate the accuracy of the measured tire contact area or the estimated vehicle weight, the percent error is defined as follows:

$$\textit{percent error} = 100\% \cdot \frac{(V_C - V_A)}{V_A} \tag{3}$$

Where V_A is the true value of the tire contact area or vehicle weight, and V_C is the estimated contact area or vehicle weight.

In addition to the percent error, the mean absolute percentage error (MAPE) from multiple tests is also evaluated, which is defined as

$$MAPE = 100\% \cdot \left\{ \frac{1}{n} \cdot \sum_{t=1}^{n} \frac{|V_C - V_A|}{V_A} \right\} \tag{4}$$

where n is the number of tests performed.

Table 2
Tire technical data.

Brand	Model	Identifier	Section Width	Aspect Ratio	Construction	Rim Diameter	Rim Width	Overall Diameter	Tread Width	Inflation Pressure
KUMHO	KMA 02	445/65R22.5	445 mm	65	Radial	22.5 in	13 in	45.9 in	13 in	120 psi

3.1. Computer vision-based measurement of tire contact area

An experiment was first carried out to investigate the accuracy of the contact area computed based on the tire contact length and tire deflection measured by the computer vision system, according to the three methods in Table 1. Fig. 8 shows the SUV used for this study, which was a 2015 Jeep Wrangler Unlimited Sahara. Jeep was selected for this experimental evaluation, because it has a similar body-on-frame chassis construction to a truck, and the shapes of its tire footprints are similar to those of truck tire footprints.

As reference, the true value of the contact area was obtained using the paint spray method, as depicted in Fig. 9. The vehicle was parked with each of the tires on a piece of white paper. The dark spray paint outlines the contact area of the tire on the paper, as shown in the Fig. 9. The tire footprint on the paper was photographed and processed to extract the true value of the tire-roadway contact area.

More specifically the photo was converted into black and white binary as demonstrated in Fig. 9. The nonzero elements in the binary image were identified, which principally represent the white area (i.e. the tire contact area) in the binary image. Utilizing the SF defined in Eq. (2) using the known dimensions of the paper, the contact area in real world physical unit was calculated. The procedure was then repeated for all for tire. These true values of the contact area are used as references.

Meanwhile, for each of the tire, its contact length and deflection were measured from images taken by the computer vision-based system. Three images were taken for each tire, and the average of the measured values was taken. Using the measured tire contact length and deflection values, the tire contact area was computed according to the three different methods (i.e., the rectangular, the deflection, and the oval methods, as detailed in Table 1. For the rectangular method, the tire width is required, and the thread width (7.5 in.) provided by the tire manufacturer is used.

Fig. 8. Image of test vehicle—2015 Jeep wrangler.

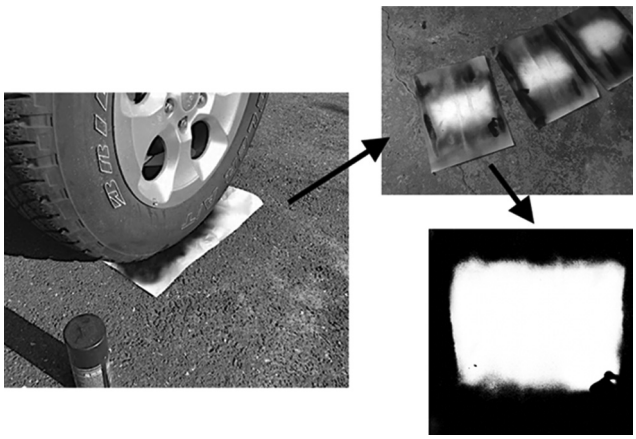

Fig. 9. Schematic of paint spraying method.

Table 3 tabulates the thus computed contact areas, in comparison with the reference true values (from the paint spraying method). The notations for the tires are front left (FL), front right (FR), rear left (RL), and rear right (RR). Table 3 also presents the percent error of the contact area of each tire measured by the computer vision system in comparison with the reference value. In addition, the MAPE of all the test tires is also listed in the table.

The contact areas computed using the computer vision measurements agree very well with the reference values. In particular, the rectangular and the deflection methods reproduced accurate contact areas, with MAPE being 1.70% and 2.37%, respectively. The oval method also gives acceptable accuracy, with MAPE of 4.21%. Considering that the deflection and the oval methods do not require the tire width information, they do have advantage over the rectangular method. It is noteworthy that the contact areas of an SUV tire are typically rounded rectangles or a racetrack shape, which are between oval and rectangular.

3.2. Computer vision-based WIM of an SUV

The accuracy of the computer vision-based vehicle weight estimation was further evaluated on the above SUV. Following the procedure described in Section 2 and Fig. 2, the weight of the vehicle was estimated respectively when the vehicle was stationary and moving at approximately 15 mph. For each of the tires, the tire contact length and tire defection were measured by the prototype computer vision system. Using the measurements, the tire contact area was calculated by the three different methods described in Table 1. For the stationary vehicle state, the tire contact area was also measured by the paint spraying method. The tire pressure data were streamed from the on-board TPMS. The manufacturer-provided curb weight of 4397 lb. was used as the true value (the reference).

Table 4 presents the estimated weights at the stationary and in-motion states, in comparison with the true value. Error of the estimated weight is also quantified for each vehicle state and each tire area computing method. Note that the weights listed in Table 4 estimated from the moving vehicle have subtracted 120 lb. to account for the weight of the driver. From Table 4, it is observed that the computer vision-based non-contact WIM system produced highly accurate weight estimates. In particular, when the rectangular method was used to compute the tire contact area based on the measured contact length, the error was −0.60% for the stationary vehicle and −1.10% for the moving vehicle. The oval method had the largest error 4.75%, which is still considered acceptable, particularly in consideration of its benefit of not requiring the tire width information.

Table 5 compares the vehicle weights estimated when the vehicle was stationary and in motion. The absolute difference and the percent difference are also computed. Table 5 suggests that there is no noticeable difference in the estimated vehicle weights between the two states. The deflection method produced the least difference, 0.09%, between the two states.

3.3. Computer vision-based WIM of heavy trucks

The non-contact WIM methodology, along with the computer vision system, was further evaluated by field experiments on heavy concrete trucks. The experiments were conducted on the side of a public road outside a concrete mixing facility where empty trucks were reloaded. The concrete facility is equipped with a static weighing station where all concrete trucks were loaded, checked

Table 3
Calculated contact area.

Method	FL		FR		RL		RR		MAPE
	Area(in^2)	Error (%)	Area(in^2)	Error (%)	Area(in^2)	Error (%)	Area(in^2)	Error (%)	
Paint spraying method	30.79	–	31.85	–	28.01	–	29.65	–	
Rectangular method	30.94	0.48%	31.41	−1.39%	29.06	3.76%	30.00	1.18%	1.70%
Deflection method	31.59	2.59%	31.59	−0.83%	27.93	−0.28%	27.93	−5.79%	2.37%
Oval method	32.55	5.72%	33.55	5.33%	28.73	2.56%	30.61	3.24%	4.21%

Table 4
Vehicle estimated weights comparing with curb weight—stationary vs. in motion.

Method	Stationary Weight (lb.)	% Error	In Motion Weight (lb.)	% Error
Curb weight	4397.00	–	4397.00	–
Rectangular	4370.63	−0.60%	4348.70	−1.10%
Deflection	4285.34	−2.54%	4289.37	−2.45%
Oval	4515.66	2.70%	4605.78	4.75%
Paint	4330.86	−1.50%	–	–

Table 5
Vehicle weight differences—stationary vs. in motion.

Method	Stationary Weight (*lb.*)	In Motion Weight (*lb.*)	Difference (*lb.*)	% Diff.
Rectangular	4370.63	4348.70	−21.92	−0.50%
Deflection	4285.34	4289.37	4.03	0.09%
Oval	4515.66	4605.78	90.12	2.00%

for proper tire inflation pressure, and weighed before exiting to the nearby public road. The tire-roadway contact lengths and the tire deflections were measured by the computer vision system and the weights were estimated for both empty and fully-loaded trucks.

The camera system was set up on the roadside at a distance approximately 20 ft away from the moving concrete trucks. The height of the camera lens was approximately 1.5 ft. from the ground, aiming at the center of the wheel with the camera optical axis perpendicular to the wheel surface plane. The concrete trucks were traveling approximately 25 mph on the road when the tire images were captured by the camera at a shutter speed of 1/8000. Images of the tires were taken from one side of the truck assuming symmetrical weight distribution. The images were then rectified to correct perspective errors and distortions before estimation of the deformation parameters for each tire. It is noteworthy that some heavy trucks utilize dual wheel system (DWS) at the rear axles. The differences between single wheel system (SWS) and DWS are quite noticeable. The SWS usually has a positive rim offset whereas the DWS generally has a negative offset, as shown in Fig. 10. Additionally, the tires used in SWS normally have an aspect ratio of 65 to 80 while aspect ratio for tires used in DWS are often 85 to 90. Though some research has suggested tire tear and wear may cause uneven load distribution on two tires of the DWS, proper periodic vehicle inspection and maintenance can tackle this problem accordingly [44–46]. Therefore, it is assumed that the inner tire of the DWS has identical contact area to the outer tire. In the case that the truck axle is a DWS, the contact area for each wheel of that axle measured is multiplied by 2.

Table 6 tabulates the tire deformation parameters, including the tire-roadway contact lengths and tire vertical deflections, measured by the computer vision system for the front, middle, and rear tires of the test concrete truck when it was empty (i.e., unloaded) and fully-loaded. It is clearly observable that the loaded concrete significantly deformed the truck tires, approximately doubling the tire-roadway contact lengths and the tire deflections. Fig. 11 shows an example of a tire (Bridgestone M860A 315/80R22.5) from empty and a fully-loaded concrete trucks.

Using the measured tire contact lengths and the tire deflections, the truck weights were estimated for the empty and fully-loaded

Table 6
Tire parameters (contact length and tire deflection) measured—unloaded vs. Loaded.

	Empty	Loaded	Difference
	Contact Length (in.)		
Front	3.30	7.67	4.37
Middle	3.25	5.40	2.15
Rear	3.99	6.25	2.26
	Tire Deflection (in.)		
Front	0.54	1.75	1.21
Middle	0.78	1.33	0.54
Rear	0.80	1.12	0.33

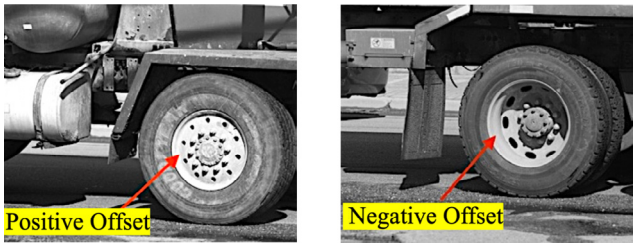

Fig. 10. SWS—positive offset (Left) vs. DWS—negative offset (Right).

Fig. 11. Concrete truck tire Bridgestone M860A—empty vs. fully-loaded.

concrete trucks. The corresponding manufacturer recommended tire pressure value (i.e., 120 psi) was used for each tire, because the tire inflation pressure is properly checked and maintained at the suggested value before the departure of the concrete trucks. Table 7 shows the estimated weights using the contact areas computed by the rectangular and the deflection method. Heavy truck tire footprints are usually in rectangular shapes, so the oval method was not used to compute the truck tire contact area.

In order to evaluate the accuracy of the weight estimates, the difference between the fully-loaded and empty truck weight estimates are compared with the true weight of the loaded concrete. Therefore, the true values of the added weight to the truck should be 28350 lb. Compared with this true value, the estimate errors are listed in Table 7. The percent error is 0.86% (when using the rectangular method to compute the tire contact area), demonstrating the effectiveness in measuring the changes in the tire deformation parameters (i.e., contact length and tire deflection) due to additional weight and high accuracy of the computer vision-based non-contact WIM system in estimating both the added concrete weight.

Numerous tests were conducted on additional three fully-loaded and four empty concretes trucks, in order to further evaluate the weight estimation accuracy of the computer vision-based non-contact WIM system. The actual weights of the fully-loaded trucks measured by the static weighing station in the concrete mixing facility were used as the true values. The fully-loaded concrete trucks were weighed immediately prior to the entrances onto the public roads. For empty trucks, the manufacturer curb weight of the Terex Concrete Mixer (37500 lb.) was used as the true value. The concrete trucks were traveling at approximately 25 mph.

For the three fully-loaded trucks, Table 8 compares their weights estimated by the computer vision-based non-contact WIM system with the true values obtained from static weighing. The percent errors are calculated for each truck. The MAPE is also computed for all the three trucks. Table 9 presents the data and analysis for the four empty trucks.

The results in Tables 8 and 9 demonstrate high degree of accuracy that the computer vision-based non-contact WIM system has achieved in estimating the weights of heavy trucks, fully-loaded or empty. For instance, the vehicle weight estimated by using the measured tire contact area (based on the rectangular method) had very low percent errors in comparison with the true values. The MAPE is only 1.21% for the fully-loaded trucks and 3.19% for the unloaded trucks. Similarly, weight estimation using the tire vertical deflection measurement (based on the deflection method) also achieved satisfactory accuracy. Furthermore, comparing Tables 8 and 9, it is observed that the computer vision-based non-contact WIM system produced more accurate weight estimates for the fully-loaded trucks than the empty ones. This might be caused by the uncertainties in the true weight of the empty trucks (i.e., the manufacturer curb weight).

3.4. Remarks

From the experiments conducted, it can be interpreted that the tire deformation parameters (i.e., the tire contact lengths and tire deflections) measured by the non-contact computer vision system produced accurate estimates of the vehicle weights in all the experiments. For computing the tire-roadway contact area, the rectangular method achieved the best agreement with the true values, i.e., the highest degree of accuracy. The deflection method, which requires only the tire vertical deflection measurement, offers simplicity over the rectangular method (that requires both the tire contact length and width.) Therefore, for implementation of the proposed WIM methodology, it is recommended to measure both the tire contact length and tire deflection and to use both of the rectangular and the deflection methods for computing the tire contact area for weight estimation. Further study can investigate if the values obtained from these two methods can be weighted to achieve high level of accuracy and reliability in vehicle weight estimation.

For field implementation, various outdoor conditions can cause errors in computer vision-based measurement. Difficult camera positions and camera vibration can cause image distortion. Poor lighting and shadowing make it difficult to identify tire-roadway contact lines that are needed for the tire deformation measurement. Errors in computing the scaling factor will also result in

Table 7
Vehicle weight comparison—unloaded vs. loaded.

Method	Empty (lb.)	Loaded (lb.)	Difference (lb.)	Error (%)
Rectangular	36207.09	64802.03	28594.94	0.86%
Deflection	34294.30	62238.90	27944.60	−1.43%

Table 8
Weight estimate of fully-loaded concrete trucks.

	Truck 283		Truck 161		Truck 63		
Method	Weight (lb.)	Error (%)	Weight (lb.)	Error (%)	Weight (lb.)	Error (%)	MAPE
Static weighing	66500.00	–	64000.00	–	72500.00	–	–
Rectangular	65720.56	−1.17%	64802.03	1.25%	73371.14	1.20%	1.21%
Deflection	65421.43	−1.62%	62238.9	−2.75%	70471.32	−2.80%	2.39%

Table 9
Weight estimate of empty concrete trucks.

	Truck 161		Truck 129		Truck 92		Truck 219		
Method	Weight (lb.)	Error (%)	Weight (lb.)	Error (%)	Weight (lb.)	Error (%)	Weight (lb.)	Error (%)	MAPE
Curb weight	37500.00	–	37500.00	–	37500.00	–	37500.00	–	–
Rectangular	36207.09	−3.45%	36877.22	−1.66%	36838.96	−1.76%	36492.78	−2.69%	3.19%
Deflection	34294.30	−8.55%	35890.57	−4.29%	36362.45	−3.03%	36185.98	−3.50%	6.46%

measurement errors. High vehicle speeds may cause motion blur in tire images. All these issues will be addressed in future work.

4. Conclusion

To address the unmet need for weighing vehicles, particularly heavy trucks, in motion, the authors have developed an innovative method for non-contact WIM by applying computer vision to extract essential tire deformation parameters (i.e., the tire-roadway contact length and tire vertical deflection). The tire-roadway contact force is computed by multiplying the tire contact pressure with the tire contact area, which can be computed by the rectangular or the deflection method using the measured tire deformation parameters.

A proof-of-concept study is presented in this paper, in which a number of field experiments were carried out on seven concrete trucks (fully loaded or empty) and an SUV, using the computer vision system assembled by the authors. The measured tire contact lengths/deflections in pixels length were converted to physical dimensions using a scaling factor obtained by identifying the known dimension in the image. Comparing the tire-roadway contact areas computed using the measured tire deformation parameters with the values produced by the paint spray method, the accuracy of the computer vision measurements has been demonstrated. Furthermore, the estimated vehicle/truck weights agreed well with their true reference values produced by static weighing or provided by the manufacturer, for both stationary and moving vehicle/trucks. For the trucks traveling at 25 mph, the truck motion did not affect the accuracy of the weight estimation.

Based on the limited number of experiments conducted in this study, both the rectangular and deflection methods have produced highly accurate estimates of tire contact areas and vehicle/truck weights. For example, for the moving concrete trucks, the mean absolute percent error in their weight estimation was only 1.21% in comparison with the true weights produced by the static weighing station. The rectangular method, which requires measurement of the tire-roadway contact length and extraction of the tire width from the tire marks, has produced a slightly higher accuracy than the deflection method. However, the deflection method requires only the tire vertical deflection measurement and thus offers simplicity and a more efficient implementation. To enhance the WIM reliability and accuracy, it is recommended to apply both of the methods to compute the tire-roadway contact area by measuring both tire contact lengths and vertical deflections.

This proof-of-concept study has developed the analytical framework, along with a computer vision system and experimentally demonstrated the feasibility of the computer vision-based non-contact WIM method. The accuracy of this method will be further evaluated in the future using a statistically meaningful sample size of trucks. Future study will also address difficult weather, field conditions, and camera resolution that may degrade image quality and affect the computer vision measurement accuracy.

CRediT authorship contribution statement

Maria Q. Feng: Conceptualization, Methodology, Supervision, Writing - review & editing, Visualization. **Ryan Y. Leung:** Formal analysis, Methodology, Data curation, Writing - original draft, Writing - review & editing, Software. **Casey M. Eckersley:** Writing - review & editing.

Declaration of Competing Interest

The authors declare that they have no known competing financial interests or personal relationships that could have appeared to influence the work reported in this paper.

References

[1] G. Fu, O. Hag-Elsafi, Vehicular overloads: load model, bridge safety, and permit checking, J. Bridg. Eng. 5 (1) (2000) 49–57.
[2] K. Wardhana, F.C. Hadipriono, Analysis of recent bridge failures in the united states, J. Perform. Constr. Facil. 17 (3) (2003) 144–150.
[3] B. Jacob, V. Feypell-de La Beaumelle, Improving truck safety: potential of weigh-in-motion technology, IATSS Res. 34 (1) (2010) 9–15.
[4] J. Richardson, S. Jones, A. Brown, E.J. O'Brien, D. Hajializadeh, On the use of bridge weigh-in-motion for overweight truck enforcement, Int. J. Heavy Veh. Syst. (2014).
[5] Y. Yu, C.S. Cai, L. Deng, State-of-the-art review on bridge weigh-in-motion technology, Adv. Struct. Eng. 19 (9) (2016) 1514–1530.
[6] D. Cebon, Design of multiple-sensor weigh-in-motion systems, Proc. Inst. Mech. Eng. Part D J. Automob. Eng. 204 (2) (1990) 133–144.
[7] R. Bushman, A. Pratt, Weigh In Motion Technology – Economics and Performance, Charlotte, NC, 1998.
[8] I. Al-Qadi, H. Wang, Y. Ouyang, K. Grimmelsman, J. Purdy, LTBP Program's Literature Review on Weigh-in-Motion Systems, 2016.
[9] F. Moses, Weigh-in-motion system using instrumented bridges, Transp. Eng. J. ASCE 105 (3) (1979) 233–249.
[10] M. Lydon, S.E. Taylor, D. Robinson, A. Mufti, E.J.O. Brien, Recent developments in bridge weigh in motion (B-WIM), J. Civ. Struct. Heal. Monit. 6 (1) (Feb. 2015) 69–81.
[11] J. Kalin, A. Žnidarič, I. Lavrič, Practical implementation of nothing-on-the-road bridge weigh-in-motion system, in: Proceedigs of the 9th International Symposium on Heavy Vehicle Weights and Dimensions, 2006, vol. 207, pp. 3–10
[12] E. O'Brien, A. Žnidarič, T. Ojio, Bridge weigh-in-motion - latest developments and applications world wide, in: International Conference on Heavy Vehicles HVParis 2008, Hoboken, NJ, USA: John Wiley & Sons, Inc., 2008, pp. 39–56.
[13] D. Feng, M.Q. Feng, Computer vision for SHM of civil infrastructure: from dynamic response measurement to damage detection – a review, Eng. Struct. 156 (2018) 105–117.
[14] T.R. McKay, C. Salvaggio, J.W. Faulring, G.D. Sweeney, Remotely detected vehicle mass from engine torque-induced frame twisting, Opt. Eng. 56 (6) (2017) 063101.
[15] C. Caprani, E. Obrien, S. Blacoe, Vision systems for analysis of congested traffic, IABSE Symp. Rep. 99 (12) (2013) 432–433.
[16] T. Ojio, C.H. Carey, E.J. OBrien, C. Doherty, S.E. Taylor, Contactless bridge weigh-in-motion, J. Bridg. Eng. 21 (7) (2016) 04016032.
[17] A. Gent, J. Walter, Pneumatic Tire. Mechanical Engineering Faculty Research, vol. 854, 2006
[18] M. Guiggiani, The Science of Vehicle Dynamics, Netherlands Springer, 2014.
[19] F. Frank, W. Hofferberth, Mechanics of the Pneumatic Tire, Rubber Chem. Technol. 40 (1) (1967) 271–322.
[20] F. Martin, Theoretische Untersuchungen zur Frage des Spannungszustandes im Luftreifen bei Abplattung, Jahrb. der Dtsch. Luftfahrfforsch. I, no. 470, 1939.
[21] Y. Pedro, Truck tire types and road contact pressures, in: Second International Symposium on Heavy Vehicle Weights and Dimensions, 1989.
[22] U. S. D. of Transportation, Tire pressure monitoring system, 2005.
[23] A.A. Ogunwemimo, Economic Analysis of Continuous Monitoring of Commercial Truck Tire Pressure Using Tire Pressure Monitoring Systems (TPMS) and RFID Economic Analysis of Continuous Monitoring of Commercial Truck Tire Pressure Using Tire, 2011.
[24] A. Vasanthara, K. Krishnamoorthy, Tire pressure monitoring system using SoC and low power design, Circ. Syst. 07 (13) (2016) 4085–4097.
[25] A.G. Ramos, E. Silva, J.F. Oliveira, A new load balance methodology for container loading problem in road transportation, Eur. J. Oper. Res. 266 (3) (May 2018) 1140–1152.
[26] S. K. Clark. Mechanics of Pneumatic Tires, vol. 1. University of Michigan, Washington, DC 20590, 1981.
[27] Smithers, "Footprint." [Online]. Available: https://www.smithersrapra.com/testing-services/by-sector/automotive/tire-testing/footprint. Accessed: 12-Jan-2018.
[28] S. K. Upadhyaya, D. Wulfsohn, Relationship between tire deflection characteristics and soil-tire contact area, American Society of Agricultural Engineers (Microfiche collection) (USA), no. 80–1005. St. Joseph, MI, 1988.
[29] M.I. Lyasko, The determination of deflection and contact characteristics of a pneumatic tire on a rigid surface, J. Terramech. 31 (4) (1994) 239–246.
[30] I. Ksenevich, V. Skotnikov, M. I. Lyasko, Undercarriage Systems, Soil, Crops. Agropromizdat, Moscow, 1985.
[31] E.J. Yoder, M.W. Witczak, Principles of Pavement Design, Wiley, 1974.
[32] D. Feng, M.Q. Feng, Experimental validation of cost-effective vision-based structural health monitoring, Mech. Syst. Sig. Process. 88 (2017) 199–211.
[33] D. Feng, M. Feng, E. Ozer, Y. Fukuda, A vision-based sensor for noncontact structural displacement measurement, Sensors 15 (7) (Jul. 2015) 16557–16575.
[34] Federal Register: Tire Safety Information, 2002.
[35] Y. Shinmura, Tire and Rim Combination, US Patent 5111865, 1992.
[36] Japanese Industrial Standard, Contours of Rims for Automobiles. Japanese Standards Association, 1989.
[37] Hankook Tire Group, Truck & Bus Tyre Technical Manual Rim & Accessories, 2018.
[38] T. Mori, J. Terramech. 29 (4) (1992) 465–475.

[39] Continental Tire North America Inc., Commercial Vehicle Tires Technical Data Book, 2015.
[40] R.W. Rivers, Tire failures and evidence manual: for traffic accident investigation, Charles C Thomas, Springfield, 2001.
[41] J.Y. Wong, Theory of Ground Vehicles, 3rd ed., John Wiley, 2001.
[42] V. Hildebrand, Radial tire with tread pattern having four or five circumferential ribs, US Patent 7207364B2, 2007.
[43] F. Puhn, How to Make Your Car Handle, HPBooks, New York, 1976.
[44] M. De Beer, C. Fisher, Stress-In-Motion (SIM) system for capturing tri-axial tyre–road interaction in the contact patch, Measurement 46 (7) (Aug. 2013) 2155–2173.
[45] USDOT, U.S. Code of Federal Regulations (CFR)-Part 396.3-Inspection, Repair, and Maintenance. 1979.
[46] M. de Beer, I. Sallie, An appraisal of mass differences between individual tyres, axles and axle groups of a selection of heavy vehicles in South Africa, in: International Conference on Weigh-In-Motion: ICWIM6 (organized with NATMEC 2012), Dallas, Texas, 2012, pp. 514–523.